

# Exploiting Cyclic Symmetry in Convolutional Neural Networks

Sander Dieleman  
 Jeffrey De Fauw  
 Koray Kavukcuoglu  
 Google DeepMind

SEDIELEM@GOOGLE.COM  
 DEFAUW@GOOGLE.COM  
 KORAYK@GOOGLE.COM

## Abstract

Many classes of images exhibit rotational symmetry. Convolutional neural networks are sometimes trained using data augmentation to exploit this, but they are still required to learn the rotation equivariance properties from the data. Encoding these properties into the network architecture, as we are already used to doing for translation equivariance by using convolutional layers, could result in a more efficient use of the parameter budget by relieving the model from learning them. We introduce four operations which can be inserted into neural network models as layers, and which can be combined to make these models partially equivariant to rotations. They also enable parameter sharing across different orientations. We evaluate the effect of these architectural modifications on three datasets which exhibit rotational symmetry and demonstrate improved performance with smaller models.

## 1. Introduction

For many machine learning applications involving sensory data (e.g. computer vision, speech recognition), neural networks have largely displaced more traditional approaches based on handcrafted features. Such features require considerable engineering effort and a lot of prior knowledge to design. Neural networks however are able to automatically extract a lot of this knowledge from data, which previously had to be incorporated into models using feature engineering.

Nevertheless, this evolution has not exempted machine learning practitioners from getting to know their datasets and problem domains: prior knowledge is now encoded in the architecture of the neural networks instead. The most prominent example of this is the standard architecture of convolutional neural networks (CNNs), which typically consist of alternating convolutional layers and pooling layers. The convolutional layers endow these models

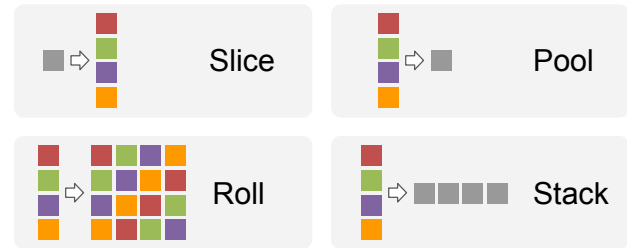


Figure 1. Visualisation of the four operations that constitute our proposed framework for building rotation equivariant neural networks.

with the property of translation *equivariance*: patterns that manifest themselves at different spatial positions in the input will be encoded similarly in the feature representations extracted by these layers. The pooling layers provide local translation invariance, by combining the feature representations extracted by the convolutional layers in a way that is position-independent within a local region of space. Together, these layers allow CNNs to learn a hierarchy of feature detectors, where each successive layer sees a larger part of the input and is progressively more robust to local variations in the layer below.

CNNs have seen widespread use for computer vision tasks, where their hierarchical structure provides a very strong prior that is especially effective for images. They owe their success largely to their scalability: the parameter sharing implied by the convolution operation allows for the capacity of the model to be used much more effectively than would be the case in a fully connected neural network with a similar number of parameters, and significantly reduces overfitting. It also enables them to be used for very large images without dramatically increasing the number of parameters.

In this paper, we investigate how this idea can also be applied to rotation invariance and equivariance. Many types of data exhibit these properties, and exploiting them to increase parameter sharing may allow us to further regularise and scale up neural networks. We propose four new neural

network layers, represented in Figure 1, which can be used together to build CNNs that are partially or fully rotation equivariant. The resulting framework is scalable and easy to implement in practice.

## 2. Cyclic symmetry

Filters in CNN layers learn to detect particular patterns at multiple spatial locations in the input. These patterns often occur in different orientations: for example, edges in images can be arbitrarily oriented. As a result, CNNs will often learn multiple copies of the same filter in different orientations. This is especially apparent when the input data exhibits rotational symmetry. It may therefore be useful to encode a form of rotational symmetry in the architecture of a neural network, just like the parameter sharing resulting from the convolution operation encodes translational symmetry. This could reduce the redundancy of learning to detect the same patterns in different orientations, and free up model capacity. Alternatively it may allow us to reduce the number of model parameters and the risk of overfitting.

There are only four possible orientations of the input that allow for the application of a filter without interpolation: the rotations over angles  $k \cdot 90^\circ$ ,  $k \in \{0, 1, 2, 3\}$ . This is because the sampling grid of an input rotated by one of these angles aligns with the original, which is not true for any other angle. We would like to avoid interpolation, because it adds complexity and can be a relatively expensive operation. If the input is represented as a matrix, the rotated versions can be obtained using only transposition and flipping of the rows or columns, two operations that are very cheap computationally. This group of four rotations is isomorphic to the cyclic group of order 4 ( $C_4$ ), and we will refer to this restricted form of rotational symmetry as *cyclic symmetry* henceforth<sup>1</sup>.

In addition to four rotations, we can apply a horizontal flipping operation, for a total of eight possible orientations obtainable without interpolation. We will refer to this as *dihedral symmetry*, after the dihedral group  $D_4$ .

We can encode cyclic symmetry in CNNs by parameter sharing: each filter should operate on four transformed copies of its input, resulting in four different feature maps. Crucially, these feature maps are not rotated versions of each other, because the relative orientation of the input and the filter is different for each of them. Note that this is equivalent to applying four transformed copies of the filter to the unchanged input. This is demonstrated in Figure 2. In this paper we will primarily use the former interpretation. We discuss the practical implications of this choice in Section 4.5.

<sup>1</sup>In literature, it is also known as ‘discrete rotational symmetry of order 4’.

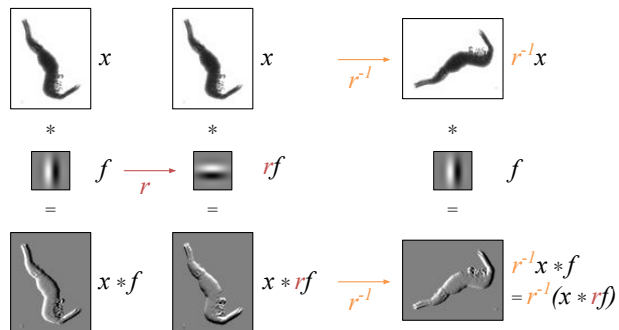


Figure 2. Convolving an image with a rotated filter (middle) and inversely rotating the result is the same as convolving the inversely rotated image with the unrotated filter (bottom). This follows from the fact that rotation is distributive w.r.t. convolution.

## 3. Equivariance and invariance

Many classes of images exhibit partial or full rotational symmetry, particularly in biology, astronomy, medicine and aerial photography. Some types of data specifically exhibit dihedral symmetry, such as board configurations in the game of Go. The tasks which we wish to perform on such data with neural networks usually require *equivariance* to rotations: when the input is rotated, the learnt representations should change in a predictable way (Lenc & Vedaldi, 2014). More formally, a function  $f$  is equivariant to a class of transformations  $\mathcal{T}$ , if for all transformations  $\mathbf{T} \in \mathcal{T}$  of the input  $x$ , a corresponding transformation  $\mathbf{T}'$  of the output  $f(x)$  can be found, so that  $f(\mathbf{T}x) = \mathbf{T}'f(x)$  for all  $x$  (Schmidt & Roth, 2012).

Often, the representations should not change at all when the input is rotated, i.e. they should be *invariant*. It follows that an invariant representation is also equivariant (but not necessarily vice versa). In this case,  $\mathbf{T}'$  is the identity for all  $\mathbf{T}$ . We also consider the special case where  $\mathbf{T}' = \mathbf{T}$ , i.e. the transformations of the input and the output are the same. We will refer to this as *same-equivariance*.

## 4. Encoding equivariance in neural nets

The simplest way to achieve (approximate) invariance to a class of transformations of the input, is to train a neural network with *data augmentation* (Simard et al., 2003): during training, examples are randomly perturbed with transformations from this class, to encourage the network to produce the correct result regardless of how the input is transformed. Provided that the network has enough capacity, it should be able to learn such invariances from data in many cases (Lenc & Vedaldi, 2014). But even if it perfectly learns the invariance on the training set, there is no guarantee that this will generalise. To obtain such a guarantee, we might want to encode the desired invariance properties in

the network architecture, and allow it to use the additional freed up learning capacity to learn other concepts. Forcing the network to rediscover prior knowledge that we have about the data is rather wasteful.

To obtain more invariant predictions from a CNN, a straightforward approach is to produce predictions for a number of different transformations of the input, and to simply combine them together by averaging them. This requires no modifications to the network architecture or the training procedure, but comes at the expense of requiring more computation to generate predictions (one inference step for each transformation considered). This approach can also be applied in the case of partial rotation invariance, or as part of a broader *test-time augmentation* strategy, which includes other transformations besides rotation over which predictions are averaged. However, as we discussed before in Section 4, it does not provide any guarantees about the invariance properties of the resulting model and it does not solve the problem in a principled way.

For the remainder of this section we will discuss the case of cyclic symmetry only (i.e. the class of transformations considered consists of the rotations over  $k \cdot 90^\circ$ ,  $k \in \{0, 1, 2, 3\}$ ), but the proposed framework can be generalised to other cases (including but not limited to dihedral symmetry).

#### 4.1. Framework

We will introduce four operations, which can be cast as layers in a neural network, that constitute a framework that we can use to easily build networks that are equivariant to cyclic rotations and share parameters across different orientations. An overview is provided in Table 1 and a visualisation in Figure 1. Each of the operations changes either the size of the minibatch (slicing, pooling) or the number of feature maps (rolling), or both (stacking). Beyond this, these operations do not affect the behaviour of the surrounding layers in any way, so in principle they are compatible with recent architectural innovations such as Inception (Szegedy et al., 2014) and residual learning (He et al., 2015).

#### 4.2. Cyclic slicing and pooling

To encode rotation equivariance in a neural network architecture, we introduce two new types of layers:

- the **cyclic slicing** layer, which stacks rotated copies of a set of input examples into a single minibatch (which is  $4\times$  larger as a result);
- the **cyclic pooling** layer, which combines predictions from the different rotated copies of an example together using a permutation-invariant pooling function

(e.g. averaging), reducing the size of the minibatch by a factor of 4 in the process.

Formally, let  $\mathbf{x}$  be a tensor representing a minibatch of input examples or feature maps, and let  $r$  be the clockwise rotation over  $90^\circ$ . The cyclic slicing operation can then be represented as  $S(\mathbf{x}) = [\mathbf{x}, r\mathbf{x}, r^2\mathbf{x}, r^3\mathbf{x}]^T$ , where we use a column vector to indicate that the rotated feature maps are stacked across the batch dimension in practice. As a result, all layers following the slicing layer will process each data point along four different *pathways*, each corresponding to a different relative orientation of the input.

Let  $\mathbf{x} = [x_0, x_1, x_2, x_3]^T$ , then we define the pooling operation  $P(\mathbf{x}) = p(x_0, r^{-1}x_1, r^{-2}x_2, r^{-3}x_3)$ , where  $p$  is a permutation-invariant pooling function, such as the average or the maximum. In practice, we find that some pooling functions work better than others, as discussed in Section 6.3.

The pooling operation can be applied after one or more dense layers, at which point the feature maps no longer have any spatial structure. In that case, the inverse rotations that realign the feature maps obtained from different pathways can be omitted. The resulting network will then be *invariant* to cyclic rotations. For some problems (e.g. segmentation) however, the spatial structure should be preserved up until the output, in which case the realignment is important. The resulting network will then be *same-equivariant*: if the input rotates, the output will rotate in the same way.

Using these two layers, it is straightforward to modify an existing network architecture to be invariant or same-equivariant by inserting a slicing layer at the input side and a pooling layer at the output. It is important to note that the effective batch size for the layers in between will become  $4\times$  larger, so we may also have to reduce the input batch size to compensate for this. Otherwise this modification would significantly slow down training.

We need not necessarily insert the pooling layer at the very end: we could also position some of the other network layers after the pooling operation, but not convolutional or spatial pooling layers. Otherwise, we would relinquish equivariance at that point: the pooled feature maps would rotate with the input (same-equivariance), which means their relative orientation w.r.t. the filters of the following layers would change.

#### 4.3. Cyclic rolling

Next, we introduce the **cyclic rolling** operation. We observe that each minibatch of intermediate activations in a network with cyclic slicing and pooling contains four sets of feature maps for each example. These are not just rota-

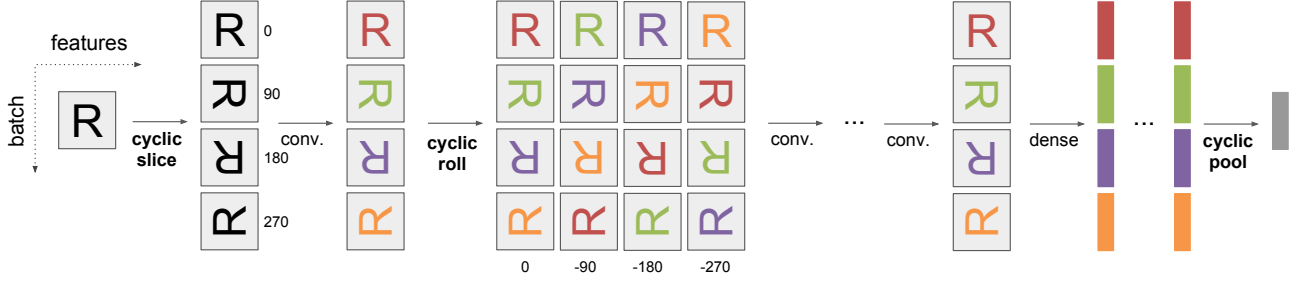


Figure 3. Schematic representation of the effect of the cyclic slice, roll and pool operations on the feature maps in a CNN. Arrows represent network layers. Each square represents a minibatch of feature maps. The letter ‘R’ is used to clearly distinguish orientations. Different colours are used to indicate that feature maps are qualitatively different, i.e. they are not rotations of each other. Feature maps in a column are stacked along the batch dimension in practice; feature maps in a row are stacked along the feature dimension.

Table 1. The four operations that form our framework for building neural networks that are equivariant to cyclic rotations. Let  $\mathbf{x} = [x_0, x_1, x_2, x_3]^T$ ,  $r$  be the clockwise rotation over  $90^\circ$ ,  $\sigma$  be a cyclic permutation shifting the elements backward, and  $p$  be any permutation-invariant pooling function.

NAME	DEFINITION	BATCH SIZE	# FEATURE MAPS
Slice	$S(\mathbf{x}) = [\mathbf{x}, r\mathbf{x}, r^2\mathbf{x}, r^3\mathbf{x}]^T$	$\times 4$	unchanged
Pool	$P(\mathbf{x}) = p(x_0, r^{-1}x_1, r^{-2}x_2, r^{-3}x_3)$	$\div 4$	unchanged
Stack	$T(\mathbf{x}) = [x_0, r^{-1}x_1, r^{-2}x_2, r^{-3}x_3]$	$\div 4$	$\times 4$
Roll	$R(\mathbf{x}) = [T(\mathbf{x}), T(\sigma\mathbf{x}), T(\sigma^2\mathbf{x}), T(\sigma^3\mathbf{x})]^T$	unchanged	$\times 4$

tions of each other, as they correspond to different relative orientations of the filters and inputs (indicated by different colours in Figure 3). By *realigning* and stacking them along the feature dimension, we can increase the number of feature maps within each pathway fourfold with a simple copy operation, which means the next convolutional layer receives a richer representation as its input. Because of this, we can reduce the number of filters in the convolutional layers while still retaining a rich enough representation. In practice, this amounts to 4-way parameter sharing: each filter produces not one, but four feature maps, resulting from different relative orientations w.r.t. the input.

To formalise this operation, we will first characterise the equivariance properties of the slicing operation  $S$ . When we apply this to a rotated input  $r\mathbf{x}$ , we obtain  $S(r\mathbf{x}) = [r\mathbf{x}, r^2\mathbf{x}, r^3\mathbf{x}, \mathbf{x}]^T = \sigma S(\mathbf{x})$ , where  $\sigma$  denotes a cyclic permutation, shifting the elements backward along the batch dimension.

We define the stacking operation  $T(\mathbf{x}) = [x_0, r^{-1}x_1, r^{-2}x_2, r^{-3}x_3]$ , which realigns the feature maps  $x_i$  corresponding to the different pathways and stacks them along the feature dimension, resulting in a row vector<sup>2</sup>.

The roll operation  $R$  then simply consists of apply-

<sup>2</sup>Note the similarity to the pooling operation, but now the realigned feature maps are stacked rather than combined together.

ing  $T$  to all possible cyclic permutations of the input, and stacking the results along the batch dimension:  $R(\mathbf{x}) = [T(\mathbf{x}), T(\sigma\mathbf{x}), T(\sigma^2\mathbf{x}), T(\sigma^3\mathbf{x})]^T$ , or equivalently,  $R(\mathbf{x}) = [\mathbf{x}, \sigma r^{-1}\mathbf{x}, \sigma^2 r^{-2}\mathbf{x}, \sigma^3 r^{-3}\mathbf{x}]$ . Figure 3 shows the effect of the cyclic slice, roll and pool operations on the feature maps in a CNN.

By stacking the feature maps in the right order, we are able to preserve equivariance across layers:  $R$  is same-equivariant w.r.t. the cyclic permutation  $\sigma$  ( $R(\sigma\mathbf{x}) = \sigma R(\mathbf{x})$ ). The resulting increase in parameter sharing can be used either to significantly reduce the number of parameters (and hence the risk of overfitting), or to better use the capacity of the model if the number of parameters is kept at the same level. In a network where a rolling layer is introduced after every convolutional layer, we can keep the number of parameters approximately constant by reducing the number of filters by half. This will in turn increase the number of produced feature maps by a factor of two, which ends up balancing out the number of parameters for each layer because it is proportional to both the number of input feature maps and the number of filters.

#### 4.4. Cyclic stacking

We may also want to achieve parameter sharing by rolling in networks that are not required to be fully equivariant: as mentioned in Section 1, even networks trained on natural images often exhibit a lot of redundancy in the fil-

ters learned in the first couple of layers. To accommodate this use case, we can simply **stack** (i.e. concatenate) feature maps obtained from the different orientations along the feature dimension, instead of pooling them together as we would otherwise. This corresponds to the stacking operation  $T$  that we introduced previously.

#### 4.5. Rotate feature maps or filters?

As mentioned in Section 2, we can equivalently rotate either the filters or feature maps on which they operate to achieve 4-way parameter sharing, because only their relative orientation affects the result of the convolution. This implies that there are two possible practical implementations, both with their own advantages and disadvantages.

Rotating the feature maps may not seem to be the most natural choice, but it is the easiest to implement in many modern deep learning software frameworks because the roll operation can be isolated and viewed as a separate *layer* in a neural network model. By stacking the feature maps corresponding to different orientations in the batch dimension, it becomes easier to exploit data parallelism (the effective batch size for most of the computationally expensive operations is larger). The feature maps must necessarily be square, otherwise it would not be possible to stack the different orientations together in a single batch. The filters need not be, however. It also implies that the roll operation has to make four copies of each feature map, which increases memory requirements.

Rotating the filters, on the other hand, means that the feature maps need not be square, but the filters must be. This operation cannot be isolated from the convolutional layers in a model, because it affects its parameters rather than the input activations. In many frameworks this complicates the implementation, and may require partial reimplementations of the convolutional layer abstraction. It only requires copying the filters, which are generally smaller than the feature maps on which they operate, so memory requirements are reduced. After training, it is straightforward to produce a version of the model that does not require any special operations beyond slicing and pooling, by stacking the different orientations of the filters for each convolutional layer. This version can then be used to perform inference on (non-square) inputs of any size.

Our choice for the former primarily stems from practical considerations (i.e. ease of implementation).

#### 4.6. Dihedral symmetry

The previous discussion readily generalises to the dihedral case, by changing the slice operation to include flipped in addition to rotated copies of the input (for a total of 8 copies), and by adapting all other operations accordingly.

One complication is that the equivariance properties of dihedral slicing are less straightforward: the resulting permutation along the batch dimension is no longer cyclic. It is also important to take into account that flipping and rotation do not commute.

## 5. Related Work

While convolutional structure has become the accepted approach of encoding translational equivariance in image representations, there is no such consensus for other classes of transformations. Many architectural modifications have been proposed to encode rotation equivariance. Schmidt & Roth (2012) modify Markov random fields (MRF) to learn rotation-invariant image priors. Kivinen & Williams (2011), Sohn & Lee (2012) and Schmidt & Roth (2012) propose modified restricted Boltzmann machines (RBMs) with tied weights to achieve rotation equivariance.

Fasel & Gatica-Perez (2006) create multiple rotated versions of images and feed them to a CNN with filters shared across different orientations. The representations are gradually pooled together across different layers, yielding a fully invariant representation at the output. Their approach of rotating the input rather than the filters is identical to ours, but our strategy for achieving invariance using a single pooling layer allows the intermediate layers to use more accurate orientation information. Dieleman et al. (2015) also create multiple rotated and flipped versions of images and feed them to the same stack of convolutional layers. The resulting representations are then concatenated and fed to a stack of dense layers. While this does not yield invariant predictions, it does enable parameter sharing across orientations. In our framework, this approach can be reproduced using a slicing layer at the input, and a stacking layer between the convolutional and dense parts of the network. A similar approach is investigated by Teney & Hebert (2016), where filters of individual convolutional layers are constrained to be rotations of each other.

Wu et al. (2015) apply rotated and flipped copies of each filter in a convolutional layer and then max-pool across the resulting activations. We concatenate them instead and prefer to pool only at the output side of the network to be able to achieve global equivariance, which is not possible if there are multiple pooling stages in the network. Indeed, they find that it is only useful to apply their approach in the higher layers of the network, and only to a subset of the filters so that some orientation information is preserved. Clark & Storkey (2015) force the filters of convolutional layers to exhibit dihedral symmetry through weight sharing, which means the resulting feature maps will necessarily be invariant. However, the network is only able to accurately detect fully symmetric patterns in the input, which is too restrictive for many problems.

Sifre & Mallat (2013) propose a model resembling a CNN with fixed rather than learned filters, which is scaling- and rotation-invariant in addition to translation-invariant. Gens & Domingos (2014) propose deep symmetry networks, a generalisation of CNNs that can form feature maps over arbitrary transformation groups.

We can also modify the architecture to facilitate learning of equivariance properties from data, rather than directly encode them. This approach is more flexible, but it requires more training data. The model of Kavukcuoglu et al. (2009) is able to learn local invariance to arbitrary transformations by grouping its filters into overlapping neighbourhoods whose activations are pooled together. Liao et al. (2013) describe a template-based approach that successfully learns representations invariant to both affine and non-affine transformations (e.g. out-of-plane rotation). Cohen & Welling (2014) propose a probabilistic framework to directly model the transformation group to which a given dataset exhibits equivariance. Tiled CNNs (Ngiam et al., 2010), in which weight sharing is reduced, are able to approximate more complex local invariances than regular CNNs.

A third alternative to encoding or learning equivariance properties involves explicitly estimating the transformation applied to the input separately for each example, as is done by transforming auto-encoders (Hinton et al., 2011) and spatial transformer networks (Jaderberg et al., 2015). This approach was also investigated for face detection by Rowley et al. (1998).

Both Goodfellow et al. (2009) and Lenc & Vedaldi (2014) discuss how the equivariance properties of representations can be measured. The latter also show that representations learnt in the lower layers of CNNs are approximately linearly transformed when the input is rotated or flipped, which implies equivariance.

## 6. Experiments

### 6.1. Datasets

We will make use of three datasets which exhibit rotational symmetry.

**Plankton** The Plankton dataset (Cowen et al., 2015) consists of 30,336 grayscale training images of varying size, divided unevenly into 121 classes which correspond to different species of plankton. We rescaled them to  $95 \times 95$  based on the length of their longest side. We split this set into separate validation and training sets of 3,037 and 27,299 images respectively. This dataset was used for the National Data Science Bowl<sup>3</sup>, a data science competition

hosted on the Kaggle platform. Although 130,400 images were provided for testing, their labels were never made public. These images were used to evaluate the competition results. We were able to obtain test scores by submitting predictions to Kaggle, even though the competition had already ended.

By nature of the way the images were acquired, the class of an organism is fully invariant to rotation: ignoring the very minor effects of gravity, the organisms may be arbitrarily oriented when they are photographed. An example image from the training set is shown in Figure 4a.

**Galaxies** The Galaxies dataset consists of 61,578 colour images of size  $424 \times 424$  for training. We downsampled them by a factor of 4 and cropped them to  $64 \times 64$ . The images display galaxies with various morphological properties and form a subset of the image used in the Galaxy Zoo 2 project (Willett et al., 2013). Each image is classified according to a taxonomy consisting of 11 questions with varying numbers of answers. There are 37 such answers in total. Questions pertain to e.g. the smoothness of the depicted galaxy, whether it has a spiral pattern and how many spiral arms there are. For each image, a vector of 37 probability values corresponding to the answers is provided, estimated from the votes of users of the Galaxy Zoo crowd-sourcing platform<sup>4</sup>. We split the dataset into a validation set of 6,157 images and a training set of 55,421 images. Since this dataset was also used for a competition on Kaggle, labels for the test set, containing 79,975 more images, were not provided. We obtained test scores by submitting predictions to Kaggle for this dataset as well.

There is no canonical orientation for galaxies in space, due to the absence of a fixed reference frame. It follows that the morphological properties of a galaxy are independent of the orientation in which we observe it from Earth. This means that the answer probabilities describing these properties should be invariant to rotation of the images. An example image is shown in Figure 4b.

**Massachusetts buildings** The Massachusetts buildings dataset (Mnih, 2013) consists of  $1500 \times 1500$  aerial images of the Boston area, with each image covering an area of 2.25 square kilometers. The dataset features 151 images, with pixelwise annotations of buildings. Following (Mnih, 2013), it was split into a training set of 137 images, a validation set of 4 images and a test set of 10 images. During training, we randomly sample smaller  $80 \times 80$  tiles and predict labels for a  $40 \times 40$  square in the center.

Because the annotations for this dataset are pixelwise, rotating an input image should result in an identical rotation of the corresponding output: the task of labeling buildings

<sup>3</sup><https://www.kaggle.com/c/datasciencebowl>

<sup>4</sup><http://www.galaxyzoo.org/>

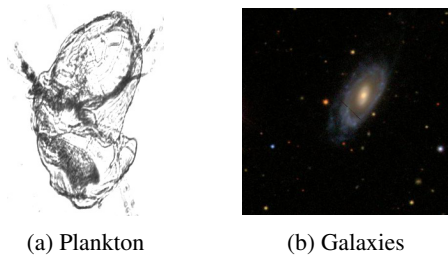


Figure 4. Example images for the Plankton and Galaxies datasets, which are rotation invariant.

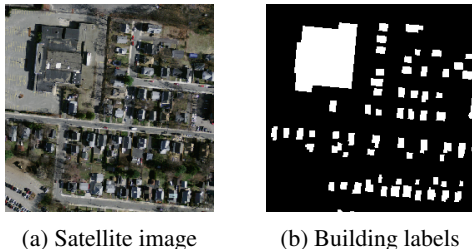


Figure 5. Example tile from the Massachusetts buildings dataset, which is same-equivariant to rotation, and corresponding labels.

in satellite images is same-equivariant. An example image and its corresponding label information from the dataset is shown in Figure 5.

## 6.2. Experimental setup

We use baseline CNNs for each dataset that were designed following today’s common practices and achieve competitive performance. For the plankton and galaxies datasets, the architectures are inspired by the VGG architectures (Simonyan & Zisserman, 2014), using  $3\times 3$  ‘same’ convolutions (which keep the spatial dimensions of the feature maps constant by zero-padding the input) throughout in combination with (overlapping) pooling. For the Massachusetts dataset, we use a stack of  $5\times 5$  ‘valid’ convolutional layers (which do not pad the input and hence reduce the spatial dimensions) without pooling, followed by  $1\times 1$  convolutions, to ensure that enough contextual information is available for each pixel. They are shown in Figure 6.

We use the Adam optimisation method (Kingma & Ba, 2014) for all experiments, because it allows us to avoid re-tuning learning rates when cyclic layers are inserted. We use discrete learning rate schedules with tenfold decreases near the end of training, following Krizhevsky et al. (2012). For the plankton dataset we also use weight decay for additional regularisation. We use data augmentation to reduce overfitting, including random rotation between  $0^\circ$  and  $360^\circ$ . We made sure to do this when training the baselines as well, such that they would have the opportunity to learn the desired invariance properties. We focus on cyclic sym-

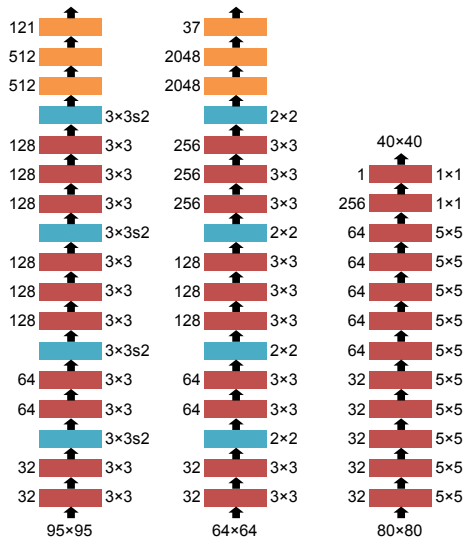


Figure 6. Baseline architectures for plankton (left), galaxies (middle) and Massachusetts buildings (right). Conv. layers are shown in red, pooling layers in blue, dense layers in orange. The numbers of units are indicated on the left, filter sizes on the right. ReLUs are used throughout. Dropout with  $p = 0.5$  is applied before all dense layers.

metry, because preliminary experiments showed that there is usually no practical benefit to dihedral symmetry. In addition, the eightfold increase in parameter sharing makes it more difficult to compare models on equal footing.

For the plankton dataset, we report the cross-entropy. For the galaxies dataset, we report the prediction root-mean-square error (*RMSE*). For the Massachusetts buildings dataset, we report the area under the ROC curve (*AUC*). We report the mean and standard deviation for these metrics across 10 training runs. We provide them for both the train and test sets, to give an idea of the level of overfitting.

Table 2. Number of model parameters and results on the plankton dataset (cross-entropy, lower is better).

MODEL	SIZE	TRAIN	TEST
baseline	2.84M	$0.4064 \pm 0.0044$	$0.7035 \pm 0.0039$
baseline $\frac{1}{2}$	0.82M	$0.5770 \pm 0.0059$	$0.7462 \pm 0.0035$
pool mean	2.84M	$0.4990 \pm 0.0115$	<b><math>0.6781 \pm 0.0041</math></b>
pool RMS	2.84M	$0.5441 \pm 0.0076$	$0.7042 \pm 0.0035$
pool max	2.84M	$0.5385 \pm 0.0127$	$0.7048 \pm 0.0057$
mean + ReLU	2.84M	$0.5376 \pm 0.0125$	$0.6982 \pm 0.0062$
RMS + ReLU	2.84M	$0.5372 \pm 0.0068$	$0.6935 \pm 0.0027$
max + ReLU	2.84M	$0.5686 \pm 0.0075$	$0.7085 \pm 0.0040$
roll all $\frac{1}{4}$	0.95M	$0.5007 \pm 0.0087$	<b><math>0.6961 \pm 0.0052</math></b>
roll dense $\frac{1}{2}$	2.28M	$0.4868 \pm 0.0106$	<b><math>0.6764 \pm 0.0041</math></b>

Table 3. Number of model parameters and results on the galaxies dataset (root-mean-square error, lower is better).

MODEL	SIZE	TRAIN	TEST
baseline	14.57M	0.08161 $\pm$ 0.00021	0.08343 $\pm$ 0.00019
baseline $\frac{1}{2}$	4.75M	0.08607 $\pm$ 0.00031	0.08710 $\pm$ 0.00025
pool mean	14.57M	0.08023 $\pm$ 0.00017	<b>0.08214</b> $\pm$ 0.00010
roll all $\frac{1}{4}$	6.84M	0.08078 $\pm$ 0.00024	<b>0.08261</b> $\pm$ 0.00017
roll dense $\frac{1}{2}$	14.57M	0.08013 $\pm$ 0.00016	<b>0.08200</b> $\pm$ 0.00009

Table 4. Number of model parameters and results on the Massachusetts buildings dataset (AUC, higher is better).

MODEL	SIZE	TRAIN	TEST
baseline	583k	0.9774 $\pm$ 0.0005	0.9714 $\pm$ 0.0005
baseline $\frac{1}{2}$	151k	0.9711 $\pm$ 0.0014	0.9643 $\pm$ 0.0011
pool mean	583k	0.9806 $\pm$ 0.0012	<b>0.9722</b> $\pm$ 0.0005
roll all $\frac{1}{4}$	158k	0.9773 $\pm$ 0.0011	<b>0.9676</b> $\pm$ 0.0008
roll all $\frac{1}{2}$	598k	0.9824 $\pm$ 0.0009	<b>0.9742</b> $\pm$ 0.0006

### 6.3. Pooling functions

First, we modified the plankton baseline architecture by adding a cyclic slicing layer at the input side, and a cyclic pooling layer just before the output layer. We reduced the batch size used for training by a factor of 4. We compared three different pooling functions: the *mean*, the maximum (*max*) and the root-mean-square (*RMS*). We also evaluated whether we should apply the *ReLU* nonlinearity to the features before pooling or not. This gives a total of six configurations, which are listed in Table 2 along with their approximate number of parameters and results.

Mean pooling without a nonlinearity gives the best results in terms of cross-entropy. We will report results using only this pooling function for further experiments, but it should be noted that the choice of function will typically depend on the dataset and the size of the model. Anecdotally, we found that alternative pooling functions sometimes result in better regularization. For the other two datasets, pooling also gives a modest improvement over the baseline.

### 6.4. Networks with rolling layers

Next, we investigated the effect of inserting one or more rolling layers into the networks, in addition to the slicing and pooling layers. We considered two approaches: in one case, we insert rolling layers after all convolutional layers, as well as after the first dense layer (*roll all*), and reduce the number of units in these layers. In the other case, we insert a rolling layer only after the first dense layer (*roll dense*). We can keep the number of feature maps constant for the layers after which rolling operations are inserted by

reducing the number of filters by a factor of 4. The layers will then have 4 times fewer parameters. When halving the number of filters instead, the number of feature maps will double relative to the original model. This implies a decrease in parameters for the layer before the rolling operation, but an increase for the next layer.

For all three datasets, we observe a limited effect on performance while the number of parameters is significantly reduced (*roll all  $\frac{1}{4}$* ). For each dataset we also report the performance of a version of the baseline network with only half the number of filters in all layers except for the last two (*baseline  $\frac{1}{2}$* ), which should have a comparable number of parameters, to demonstrate that the models with rolling layers make more efficient use of the same parameter budget. This is especially interesting because these models take roughly the same amount of computation to train; the additional cost of the roll operations is minimal compared to the cost of the convolutions.

For the plankton and galaxies datasets, the baseline models have several dense layers. The first one of these has the most parameters, because its input consists of a flattened stack of feature maps from the topmost convolutional layer. We can reduce the number of parameters in this layer by halving the number of units and adding a rolling layer (*roll dense  $\frac{1}{2}$* ). This doubles the number of parameters of the next dense layer, but for the plankton network the net result is a reduction because that layer had fewer parameters to begin with. Performance is slightly improved compared to the baseline networks.

For the Massachusetts buildings dataset, the baseline model is fully convolutional. We have evaluated a version of the network with roll layers where the number of filters in each layer is reduced only by a factor of 2 (*roll all  $\frac{1}{2}$* ), resulting in a network with roughly the same number of parameters as the baseline, but with better performance. Note that for the other datasets, which are more limited in size, such models would heavily overfit.

## 7. Conclusion and future work

We have introduced a framework for building rotation equivariant neural networks, using four new layers which can easily be inserted into existing network architectures. Beyond adapting the minibatch size used for training, no further modifications are required. We demonstrated improved performance of the resulting equivariant networks on datasets which exhibit full rotational symmetry, while reducing the number of parameters. A fast GPU implementation of the rolling operation for Theano (using CUDA kernels) is available at <https://github.com/benanne/kaggle-ndsb>.

In future work, we would like to apply our approach to



other types of data which exhibit rotational symmetry, particularly in domains where data scarcity is often an issue (e.g. medical imaging), and where additional parameter sharing would be valuable to reduce overfitting. We would also like to extend our work to volumetric data, where reducing the number of parameters is even more important and where a larger number of symmetries can be exploited without requiring costly interpolation.

## Acknowledgements

The authors would like to thank Jeroen Burms, Pieter Buteneers, Taco Cohen, Jonas Degraeve, Lasse Espeholt, Max Jaderberg, Ira Korshunova, Volodymyr Mnih, Lionel Pigou, Laurent Sifre, Karen Simonyan and Aäron van den Oord for their insights and input.

## References

- Clark, Christopher and Storkey, Amos. Training deep convolutional neural networks to play go. In *Proceedings of the 32nd International Conference on Machine Learning (ICML-15)*, pp. 1766–1774, 2015.
- Cohen, Taco and Welling, Max. Learning the irreducible representations of commutative lie groups. *arXiv preprint arXiv:1402.4437*, 2014.
- Cowen, Robert K., Sponaugle, S., Robinson, K.L., and Luo, J. Planktonset 1.0: Plankton imagery data collected from f.g. walton smith in straits of florida from 2014-06-03 to 2014-06-06 and used in the 2015 national data science bowl, 2015. (NODC Accession 0127422). NOAA National Centers for Environmental Information. Dataset. doi:10.7289/V5D21VJD.
- Dieleman, Sander, Willett, Kyle W, and Dambre, Joni. Rotation-invariant convolutional neural networks for galaxy morphology prediction. *Monthly Notices of the Royal Astronomical Society*, 450(2):1441–1459, 2015.
- Fasel, Beat and Gatica-Perez, Daniel. Rotation-invariant neoperceptron. In *Pattern Recognition, 2006. ICPR 2006. 18th International Conference on*, volume 3, pp. 336–339. IEEE, 2006.
- Gens, Robert and Domingos, Pedro M. Deep symmetry networks. In *Advances in neural information processing systems*, pp. 2537–2545, 2014.
- Goodfellow, Ian, Lee, Honglak, Le, Quoc V, Saxe, Andrew, and Ng, Andrew Y. Measuring invariances in deep networks. In *Advances in neural information processing systems*, pp. 646–654, 2009.
- He, Kaiming, Zhang, Xiangyu, Ren, Shaoqing, and Sun, Jian. Deep residual learning for image recognition. *arXiv preprint arXiv:1512.03385*, 2015.
- Hinton, Geoffrey E, Krizhevsky, Alex, and Wang, Sida D. Transforming auto-encoders. In *Artificial Neural Networks and Machine Learning–ICANN 2011*, pp. 44–51. Springer, 2011.
- Jaderberg, Max, Simonyan, Karen, Zisserman, Andrew, et al. Spatial transformer networks. In *Advances in Neural Information Processing Systems*, pp. 2008–2016, 2015.
- Kavukcuoglu, Koray, Ranzato, Marc Aurelio, Fergus, Rob, and Le-Cun, Yann. Learning invariant features through topographic filter maps. In *Computer Vision and Pattern Recognition, 2009. CVPR 2009. IEEE Conference on*, pp. 1605–1612. IEEE, 2009.
- Kingma, Diederik and Ba, Jimmy. Adam: A method for stochastic optimization. *arXiv preprint arXiv:1412.6980*, 2014.
- Kivinen, Jyri J and Williams, Christopher KI. Transformation equivariant boltzmann machines. In *Artificial Neural Networks and Machine Learning–ICANN 2011*, pp. 1–9. Springer, 2011.
- Krizhevsky, A., Sutskever, I., and Hinton, G. E. Imagenet classification with deep convolutional neural networks. In *Advances in Neural Information Processing Systems 25*, 2012.
- Lenc, Karel and Vedaldi, Andrea. Understanding image representations by measuring their equivariance and equivalence. *arXiv preprint arXiv:1411.5908*, 2014.
- Liao, Qianli, Leibo, Joel Z, and Poggio, Tomaso. Learning invariant representations and applications to face verification. In *Advances in Neural Information Processing Systems*, pp. 3057–3065, 2013.
- Mnih, Volodymyr. *Machine Learning for Aerial Image Labeling*. PhD thesis, University of Toronto, 2013.
- Ngiam, Jiquan, Chen, Zhenghao, Chia, Daniel, Koh, Pang W, Le, Quoc V, and Ng, Andrew Y. Tiled convolutional neural networks. In *Advances in Neural Information Processing Systems*, pp. 1279–1287, 2010.
- Rowley, Henry A, Baluja, Shumeet, and Kanade, Takeo. Rotation invariant neural network-based face detection. In *Computer Vision and Pattern Recognition, 1998. Proceedings. 1998 IEEE Computer Society Conference on*, pp. 38–44. IEEE, 1998.

- Schmidt, Uwe and Roth, Stefan. Learning rotation-aware features: From invariant priors to equivariant descriptors. In *Computer Vision and Pattern Recognition (CVPR), 2012 IEEE Conference on*, pp. 2050–2057. IEEE, 2012.
- Sifre, Laurent and Mallat, Stéphane. Rotation, scaling and deformation invariant scattering for texture discrimination. In *Computer Vision and Pattern Recognition (CVPR), 2013 IEEE Conference on*, pp. 1233–1240. IEEE, 2013.
- Simard, Patrice Y, Steinkraus, Dave, and Platt, John C. Best practices for convolutional neural networks applied to visual document analysis. In *null*, pp. 958. IEEE, 2003.
- Simonyan, Karen and Zisserman, Andrew. Very deep convolutional networks for large-scale image recognition. *arXiv preprint arXiv:1409.1556*, 2014.
- Sohn, Kihyuk and Lee, Honglak. Learning invariant representations with local transformations. *arXiv preprint arXiv:1206.6418*, 2012.
- Szegedy, Christian, Liu, Wei, Jia, Yangqing, Sermanet, Pierre, Reed, Scott, Anguelov, Dragomir, Erhan, Dumitru, Vanhoucke, Vincent, and Rabinovich, Andrew. Going deeper with convolutions. *arXiv preprint arXiv:1409.4842*, 2014.
- Teney, Damien and Hebert, Martial. Learning to extract motion from videos in convolutional neural networks. *arXiv preprint arXiv:1601.07532*, 2016.
- Willett, Kyle W, Lintott, Chris J, Bamford, Steven P, Masters, Karen L, Simmons, Brooke D, Casteels, Kevin RV, Edmondson, Edward M, Fortson, Lucy F, Kaviraj, Sugata, Keel, William C, et al. Galaxy zoo 2: detailed morphological classifications for 304 122 galaxies from the sloan digital sky survey. *Monthly Notices of the Royal Astronomical Society*, pp. stt1458, 2013.
- Wu, Fa, Hu, Peijun, and Kong, Dexing. Flip-rotate-pooling convolution and split dropout on convolution neural networks for image classification. *arXiv preprint arXiv:1507.08754*, 2015.